3496 © *1980 The Chemical Society of Japan* *Bull. Chem. Soc. Jpn.*, ***53***, *3496—3503 (1980)* [Vol. 53, No. 12

# Is $O_2^*(a^1\Delta_g)$ Formed in the $O+O_3$, $H+O_3$, and $NO+O_3$ Reactions?

Nobuaki Washida,* Hajime Akimoto, and Michio Okuda

*The National Institute for Environmental Studies, P.O. Tsukuba-gakuen, Tsukuba, Ibaraki 305*

(Received March 11, 1980)

An attempt was made to detect $O_2^*(a^1\Delta_g)$ in the reactions of $O+O_3$, $H+O_3$, and $NO+O_3$ using a photoionization mass spectrometer. No significant signals for $O_2^*(a^1\Delta_g)$ were observed in these reactions. From the results, it is concluded that less than 0.06, 0.001, and 0.002 of the reactive collisions result in the production of $O_2^*(a^1\Delta_g)$ in the reactions of $O+O_3$, $H+O_3$ and $NO+O_3$ respectively, all at 298 K. The failure to observed $O_2^*(a^1\Delta_g)$ in these reactions was discussed by means of correlation diagrams and GVB model representations.

Recently, the observation of the singlet oxygen formed in the reaction of hydrogen atoms with molecular oxygen was reported in our laboratory.[1] In this system it was determined that the singlet oxygen was produced by the reaction of hydrogen atoms with hydroperoxyl radicals, which had themselves been formed by the recombination reaction of hydrogen atoms with molecular oxygen:

$$H + O_2 + M \rightarrow HO_2 + M \qquad (1)$$

$$HO_2 + H \rightarrow H_2 + O_2^*(a^1\Delta_g) \qquad (2)$$

A photoionization mass spectrometer was used to detect the singlet oxygen. When an argon lamp with a LiF window is used as a light source to photoionize the molecules, singlet oxygen can be photoionized by the argon resonance lines (11.83 and 11.62 eV), but ground-state molecular oxygen can not be ionized by these lines,[1,2] since the ionization potential for ground-state molecular oxygen is 12.06 eV, and the $O_2^*(a^1\Delta_g)$ and $O_2^*(b^1\Sigma_g^+)$ states are 0.98 and 1.63 eV higher than the ground-state respectively. The detection sensitivity of the photoionization mass spectrometer to singlet oxygen is quite high in comparison with the photometric detection by means of the forbidden $O_2^*(a^1\Delta_g) \rightarrow O_2(X^3\Sigma_g^-)$ transition. The detection limit is about $10^9$—$10^{10}$ molecules $cm^{-3}$ for singlet oxygen in the reactor under good conditions (very low background signals and in the absence of the large signals around mass 32). Further, when photoionization mass spectrometry was used to detect singlet oxygen, the interference by the chemiluminescence in the reaction system was eliminated. For example, in the $H+O_2$ reaction system, singlet oxygen in the $a^1\Delta_g$ state could not be observed by the photometric method,[3] since the emission from $O_2^*(a^1\Delta_g)$ was overlapped by the strong chemiluminescence by $HO_2$. Therefore, photoionization mass spectrometry is a useful method to detect singlet oxygen in the chemiluminescent reaction system.

The reactions of $O+O_3$, $H+O_3$ and $NO+O_3$ can produce singlet oxygen according to the exothermicity and the spin correlation of the reactions. Nevertheless, this possibility has been ignored.[4] In this work, the fractions for the formation of singlet oxygen in the above reactions were determined by the use of the photoionization mass spectrometer; it seemed that this would be useful because strong chemiluminescence by OH and $NO_2$ has been observed in the near-IR region in all the above reactions except the $O+O_3$ reaction. After that, the reaction processes will be discussed using correlation diagrams and GVB model representations.

## Experimental

The experimental set-up of the fast-flow reactor is shown in Fig. 1. The photoionization mass spectrometer coupled to the fast-flow reactor is as has been described previously.[5] The inner diameter of the cylindrical Pyrex reactor tube is 12.6 mm, and the length of the reaction zone can be varied from 10 to 200 mm by sliding the inlet tube (4 mm o.d.) in an O-ring seal. Ozone enters the main flow through six radially directed holes at the end of the inlet tube.

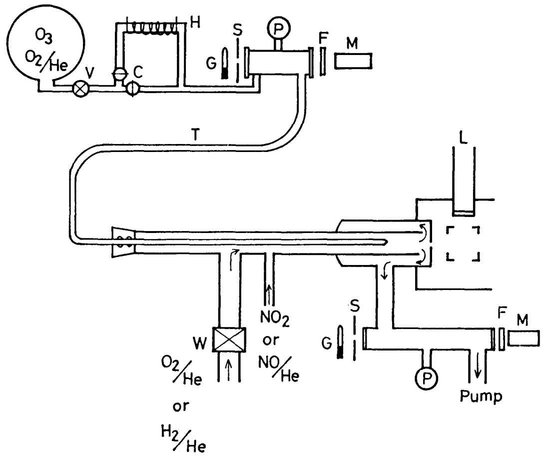

Fig. 1. Schematic diagram of the fast-flow reactor for the reactions of O, H, and NO with $O_3$.
V: Variable leak, C: Teflon stopcock, H: heater, G: Hg lamp, S: slit P: MKS baratron gauge, F: filter M: photomultiplier L: Ar lamp, T: Teflon tube, W: microwave cavity.

Hydrogen and oxygen atoms were produced in a microwave discharge (2450 MHz) in a helium mixture. The concentrations of both atoms were determined by titration with $NO_2$ according to the $H+NO_2 \rightarrow OH+NO$, and $O+NO_2 \rightarrow NO+O_2$ reactions, using the signals for NO at mass 30 as an indicator of the titration endpoint. $NO_2$ was added at a point 200 mm upstream from the sampling pinhole (the reaction time is about 10 ms under total pressure of 4 Torr (1 Torr = 133.3 Pa)). The method of determining the hydrogen-atom concentration is as has been described previously.[5] The known partial pressures of NO were added to calibrate the instrument sensitivity, typically about $2\times10^4$ counts/s for 1 mTorr of NO when two new argon lamps were used. Since the intensity of the argon lamps decreased slowly as a result of the origination of a color center in the LiF windows, the lamps were changed every 20 h. The measurements were then done between 10 to 20 h after the start of the discharge of the new lamps, because in this period the intensity of the lamp was fairly stable.

The total and partial pressures of the gases were measured with an MKS Baratron gauge and were corrected to the values at the pinhole, considering the effect of the small pressure drop down the reactor tube.[5] Furthermore, the partial pressures of each component gas were corrected by means of the flow equation.[5] The linear-flow velocity, as measured with a bubble meter, was 16.5 m $s^{-1}$ at 2 Torr, 19.9 m $s^{-1}$ at 4 Torr, and 21.4 m $s^{-1}$ at 6 Torr at 298 K. In this case, the flow in the flow tube, $F$ (Torr l $s^{-1}$), as a function of the total pressure, $P$ (Torr), was given by this equation: $F(P)=0.192+2.001P+0.0919P^2$. In this study, experiments were done under a total pressure of about 4 Torr.

The gases, $H_2$ (Nippon Sanso, 99.9999%), $O_2$ (Nippon Sanso, 99.99%), He (Nippon Sanso, 99.9999%), and $NO_2$ (Matheson, 99.5%), were used without further purification. The NO (Matheson, 99.0%) was purified by passing it through a column of Ascarite and was then distilled bulb-to-bulb using liquid nitrogen traps. After this purification, the amount of $NO_2$ present in this purified NO was less than 0.01%.[5] The ozone was prepared from a commercial ozonizer and was trapped on 500 grams of liquid nitrogen-cooled silica gel (5—10 mesh). After pumping, the adsorbed mixture of $O_3$ and $O_2$ on silica gel was heated up to room temperature and stored in a 50-l flask with a helium diluent. The mixture obtained usually consisted of 2—10% ozone and 10—20% oxygen in helium. The concentration of ozone was measured by absorption photometry at positions upstream and downstream of the flow reactor using a quartz cell, a Hg lamp coupled with a 2540 Å filter, and a photomultiplier.

The ozone was added to the reactor through a movable inlet. The measurements were done in both the presence and absence of ozone. In the case without $O_3$, the mixture of $O_3$–$O_2$–He was passed through a heated quartz tube (about 800 °C). In this case, the ozone was decomposed completely and converted to $O_2$ (no O atoms or no $O_3$ were detected by mass spectrometry and UV absorption). Switching the conditions with ozone and without ozone by means of Teflon stopcocks, the change in the signal at mass 32 was measured. The concentration of $O_2$ which was contained initially in the $O_3$–$O_2$–He mixture, $[O_2]_i$, was determined as follows. The $O_3$–$O_2$–He mixture was passed through the heated quartz tube. Under the condition without ozone, molecular oxygen was reacted with hydrogen atoms, and the singlet oxygen was produced as has been described before. Since the fraction of Reaction 2 in the total reaction of $HO_2$+H was determined[1] to be 0.015±0.003, the concentration of $O_2$,

$$[O_2] = [O_2]_i + 3/2[O_3], \qquad \text{(I)}$$

could be calculated using the rate constant for Reaction 1, the concentration of the hydrogen atoms, the total pressure, the reaction time, and the concentration of the singlet oxygen produced:

$$[O_2] = \frac{[O_2^*(a^1\Delta_g)]}{0.015\,k_1[H]t}, \qquad \text{(II)}$$

where it is assumed that the rate for Reaction 2 is very rapid and that the concentration of $HO_2$ is in a steady-state concentration.[1] When the value for $[O_2]$ is determined, the $[O_2]_i$ can be calculated by means of Eq. I.

The flowing gases were sprayed through a conical Pyrex pinhole (0.2 mm in diameter) into the ionization region of a quadrupole mass spectrometer, where a collimated light beam from a microwave-powerd discharge lamp was intersected. In this work, an argon lamp with a LiF window was used photoionize the molecules. The concentration of singlet oxygen was calculated from the relative ionization cross section for NO and $O_2^*(a^1\Delta_g)$ by means of argon-resonance lines,[6] *i.e.*, $\sigma_{O_2^*}/\sigma_{NO}=0.5$. Since the sensitivity of NO to this instrument is $2\times10^4$ counts/s for 1 mTorr of NO, $10^{-4}$ m Torr of $O_2^*(a^1\Delta_g)$ could theoretically be detected.

The ions formed by photoionization were accelerated and focused into a quadrupole mass filter (UTi Model 100C). After mass selection, the ions were counted by means of a Daly-type detector[7] operated at −20 kV, a thin aluminum-coated plastic scintillator, and pulse-counting electronics (Canberra, Multichannel Analyzer, Omega-1). A working pressure of $2\times10^{-5}$ Torr or less was maintained in the vacuum can by means of a 1200-l $s^{-1}$ oil-diffusion pump with a liquid nitrogen trap. All the measurements were done at room temperature, 298±3K.

## Results and Discussion

*1) $O+O_3$ Reaction.* The reaction of atomic oxygen with ozone is known to produce two ground-state oxygen molecules:

$$O(^3P) + O_3(X^1A_1) \rightarrow 2O_2(X^3\Sigma_g^-) \qquad \text{(3a)}$$
$$\Delta H = -93.7\ \text{kcal/mol.}$$

The vibrational excitation of ground-state oxygen[7] has been observed in levels up to $v=20$ or up to $v=25$ due to the exothermicity of Reaction 3a. However, the existence of singlet oxygen ($a^1\Delta_g$ and $b^1\Sigma_g^+$) has never been observed, although the processes to form $O_2(X^3\Sigma_g^-)+O_2^*(a^1\Delta_g)$ or $O_2^*(b^1\Sigma_g^+)$ are accessible energetically and spin-allowed:

$$O(^3P) + O_3(X^1A_1) \rightarrow O_2(X^3\Sigma_g^-) + O_2^*(a^1\Delta_g) \qquad \text{(3b)}$$
$$\rightarrow O_2(X_3\Sigma_g^-) + O_2^*(b^1\Sigma_g^+). \qquad \text{(3c)}$$

Measurements of the signals at mass number 32 were made by the addition of ozone to the oxygen atoms/He flow, which was produced in the microwave discharge of the $O_2$/He mixture. In this case, singlet oxygen was produced initially through the microwave discharge of the $O_2$/He mixture. This singlet oxygen initially produced disturbs the measurement of the signals at $m/e=32$ as a background. Therefore, measurements under the conditions of a high concentration of oxygen atoms and a low singlet-oxygen concentration in the

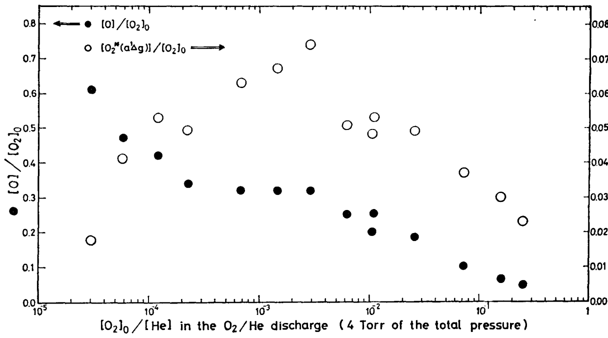

Fig. 2. The ratio of oxygen atoms produced to the initial concentration of $O_2$ in the $O_2$/He discharge, $[O]/[O_2]_0$ (●), and the ratio of singlet oxygen produced to the initial concentration of $O_2$ in the $O_2$/He discharge, $[O_2^*(a^1\Delta g)]/[O_2]_0$ (○), are plotted against the $[O_2]_0/[He]$ in the $O_2$/He mixture. Discharge was done at total pressure of 4 Torr.

$O_2$/He discharge were desired. The concentrations of the oxygen atoms and singlet oxygen produced in the discharge were measured under a variety of ratios of $O_2$ to He in the $O_2/H_2$ discharge. Figure 2 shows that the absolute concentrations of both the oxygen atoms and the singlet oxygen increased at higher values of $[O_2]_0$/[He], but the ratio of the concentration of the oxygen atoms produced to the initial concentration of $O_2$ is larger at lower values of $[O_2]_0$/[He] (*i.e.*, oxygen atoms were produced effectively at a low "initial concentration of $O_2$," $[O_2]_0$). On the other hand, the ratio of the concentration of the singlet oxygen produced to the initial concentration of $O_2$ is smaller at lower values of $[O_2]_0$/[He]. The value of $[O_2^*]/[O_2]_0$ then passed through a maximum and, after that, decreased as the value of $[O_2]_0$/[He] in increased. This decrease can be explained by the quenching of the singlet oxygen by oxygen atoms and ozone because the mixture of $O_2$ and He is discharged very far upstream of the reactor and the contact time of the discharged gases is about 50 ms. According to the results shown in Fig. 2, the condition of a low $[O_2]_0$/[He] ratio should be good for measurement because the ratio of the atomic oxygen to the singlet oxygen formed is the largest.

The mass spectra measured in the $O+O_3$ reaction system are shown in Fig. 3. As is shown in Fig. 3, the singlet oxygen was produced in the $O_2$/He discharge and the increment of the signal at $m/e=32$ was not clear when ozone was added. The signal observed at $m/e=30$ may be the signal for NO, which is produced by the nitrogen present in the $O_2$/He mixture as an impurity. The small signal at $m/e=32$ when only the $O_3$–$O_2$–He mixture was introduced ((d) in Fig. 3) can be explained by the surface ionization in the ionization chamber. The mass spectrometer was fixed at $m/e=32$, and the signals at $m/e=32$ were accumulated. The results are shown in Table 1. In this case, measurements were

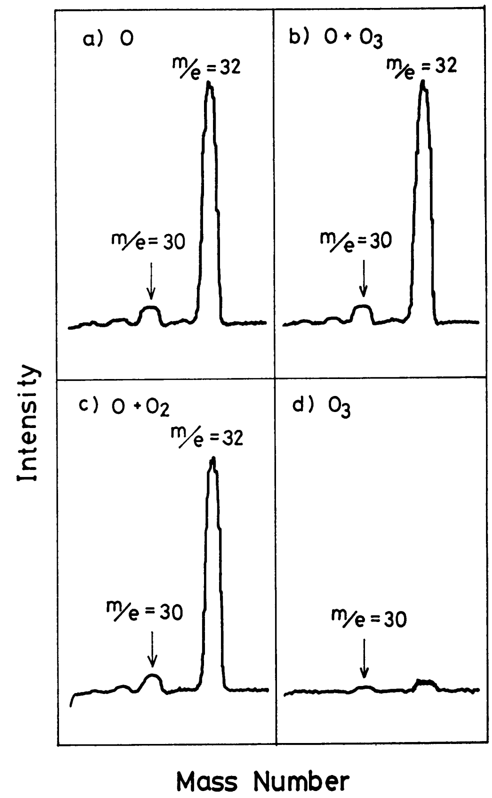

Fig. 3. Mass spectra in the $O+O_3$ reaction system. a): Only $O_2$/He discharge. b): $O_3$–$O_2$–He mixture was added to the $O_2$/He discharge. c): $O_3$–$O_2$–He mixture was passed through the heated quartz tube. Ozone was converted to $O_2$. d): Discharge was turned off. Only $O_3$–$O_2$–He mixture flowed Conditions: total pressure=4.032 Torr, $[O]_0$=4.6 m Torr $[O_3]$= 28.6 mTorr, reaction time =10.05 ms.

TABLE 1. RESULTS IN THE MEASUREMENT OF THE SIGNALS AT $m/e=32$ IN THE $O+O_3$ REACTION

| Conditions | | | | Signals at $m/e=32$ counts/5 s (± was derived from the standard deviation in the 50 measurements) | | |
|---|---|---|---|---|---|---|
| $O_2$/He discharge | Sensitivity of NO for 1 mTorr of NO | Reaction time (ms) | $O_3$–$O_2$–He Mixture added | $O_2$/He Discharge | Addition of $O_3$ ($O_3$–$O_2$–He mixture) | $O_3$ converted to $O_2$ ($O_2$–He mixture) |
| [a]<br>Total pressure, 4.043 Torr<br>$[O_2]_0$ 0.16 mTorr<br>$[O]_0$ 0.095 mTorr<br>$O_2^*(a^1\Delta_g)$ 0.003 mTorr | 18326 counts/s | 10.05 | Total: 338 mTorr<br>$[O_3]$ 29.4 mTorr<br>$[O_2]_i$ 62.5 mTorr | d. 207.3±18.1<br>nd. 69.7±10.0<br>d.−nd. 137.6±12.4 | d. 216.3±19.4<br>nd. 84.2± 9.7<br>d.−nd. 132.1±11.9 | d. 216.7±16.2<br>nd. 74.9± 8.4<br>d.−nd. 141.8±10.6 |
| [b]<br>Total pressure, 4.032 Torr<br>$[O_2]_0$ 13.8 mTorr<br>$[O]_0$ 4.6 mTorr<br>$O_2^*(a^1\Delta_g)$ 0.86 mTorr | 17458 counts/s | 10.05 | Total: 329 mTorr<br>$[O_3]$ 28.6 mTorr<br>$[O_2]_i$ 60.9 mTorr | d. 37638.9±390.6<br>nd. 103.3±9.9<br>d.−nd. 37535.6±389.5 | d. 37496.2±370.3<br>nd. 135.1±11.1<br>d.−nd. 37361.1±369.0 | d. 37594.4±353.5<br>nd. 111.3±8.5<br>d.−nd. 37483.1±352.3 |

done under two different conditions: the $[O_2]_0/[He]$ ratios in the $O_2$/He discharge were $4.0\times10^{-5}$ and $3.4\times10^{-3}$. As is shown in Fig. 2, the former is the case when the value for the ratio of the singlet oxygen to the oxygen atoms produced in the $O_2$/He discharge is small, while the latter is the case when the ratio of the singlet oxygen to the atomic oxygen has its maximum value. All the experimental conditions and signals at $m/e=32$ (counts/5 s) in the presence and absence of ozone are listed in Table 1. All the signals at $m/e=32$ were accumulated for 5 s per channel, and 50 channels were used for one measurement. The error limits ($\pm$) were derived from the standard deviation in these 50 signals. The signals at mass 32 were measured with the discharge on (d.) and off (nd.), (*i.e.*, in the presence and absence of oxygen atoms) and the difference (d. —nd.) used as the real signal for each measurement. The concentration of the singlet oxygen formed initially in the $O_2$/He discharge, listed in the first column in Table 1, was calculated from the signals at $m/e=32$ in the $O_2$/He discharge and the sensitivity of the instrument to NO. The small increment in the background (signals for nd.) when the $O_3$–$O_2$–He mixture was added can be explained by the effect of the field emission from the —20 kV stainless-steel target. As is shown in Table 1, the increase in the signals at $m/e=32$ could not be observed when the $O_3$–$O_2$–He mixture was added to the $O_2$/He discharged gases.

The rate constants for the reactions of $O+O_3$, $k_3$, have been reported to be 7.5, 8.3, and $10.6\times10^{-15}$ $cm^3$ $molecule^{-1}$ $s^{-1}$ at 300 K.8—10) If the reaction proceeds only to produce singlet oxygen (Reactions 3b or 3c), the singlet oxygen produced should be given by $k_3[O][O_3]t$. The values for $k_3[O][O_3]t$ calculated are $2.5\times10^{11}$ and $1.2\times10^{13}$ molecule/$cm^3$ in the (a) and (b) measurements respectively in Table 1. In this case, $8.3\times10^{-15}$ $cm^3$ $molecule^{-1}$ $s^{-1}$ was used at the value for $k_3$. The detectable limit, if the increment of the signals occurred in the addition of the $O_3$–$O_2$–He mixture, can be estimated to be 20 counts/5 s for the (a) measurement and 1000 counts/5 s for the (b) measurement. These values (counts/5 s) correspond to $1.4\times10^{10}$ molecule/$cm^3$ and $7.6\times10^{11}$ molecule/$cm^3$ respectively. The value for the detectable $O_2^*(a^1\Delta_g)$, divided by the value for $k_3[O]_0[O]_3t$, gives the upper limit of the fraction for the formation of singlet oxygen, Reactions 3b or 3c, in the total reaction of $O+O_3$. The fractions were calculated to be less than 0.06 in both measurements, (a) and (b). No advantage was obtained in the accuracy of the value of the fraction in the (a) measurement (with the small initial signal of $O_2^*(a^1\Delta_g)$), because the ratio of the counting error to the signal was larger in the smaller signal in this equipment.

The deactivation rate constants of $O_2^*(a^1\Delta_g)$ by $O(^3P)$, $O_2$ and $O_3$ previously reported are $\leq1.3\times10^{-16}$,11) 0.4—$2.2\times10^{-18}$,12) and $4.4\times10^{-15}$ $cm^3$ $molecule^{-1}$ $s^{-1}$ 13) respectively. These deactivation rates are quite slow. The quenching of $O_2^*(a^1\Delta_g)$ by $O(^3P)$ and $O_2$ is negligibly small, and that by $O_3$ is less than 5% of the $O_2^*(a^1\Delta_g)$ supposed to be formed in Reaction 3b. Therefore, it was concluded that the fraction for the formation of $O_2^*(a^1\Delta_g)$, Reaction 3b, in the total reaction of $O+O_3$ is less than 0.06. The deactivation rate constant of $O_2^*(b^1\Sigma_g^+)$ by $O_3$ was been reported to be fast, $7\times10^{-12}$ $cm^3$ $molecule^{-1}$ $s^{-1}$,14) This rate shows that the $O_2^*(b^1\Sigma_g^+)$ should be quenched completely under our experimental conditions if the $O_2(b^1\Sigma_g^+)$ is produced *via* Reaction 3c. Therefore, the conclusion is given only for the formation of $O_2^*(a^1\Delta_g)$, and only $O_2^*(a^1\Delta_g)$ will be dealt with in the following experiments and discussions.

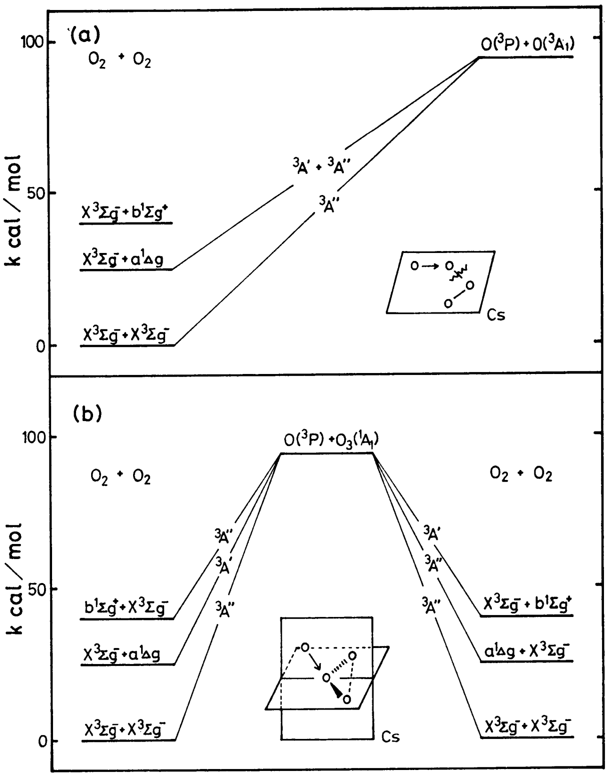

Fig. 4. Minimal state correlation diagrams in the $O+O_3$ reaction system when all atoms lie in a plane (a) and when $O(^3P)$ approaches $O_3$ in the plane which bisects the $O_3$ bond angle (b).

As has been mentioned before, vibrationally excited ground-state oxygen molecules were observed in the flash-photolysis absorption experiment.7) According to the measurement by McGrath and Norrish,7) the maximum in the population distribution of vibrationally excited $O_2$ is when $v=12$, 13, or 14, and both higher and lower levels have progressively lower populations. However, since the absorption cross-section in the Schumann-Runge band system in $O_2$ is smaller at lower $v$ levels, population distributions lower than $v=11$ could not be measured in their observation. The energy for $v=12$, 13, or 14 is about a half of the exothermic energy for the $O+O_3$ reaction, 3a, that is about 4 eV. Therefore, the formation of singlet oxygen is energetically acceptable except when the two oxygen molecules formed in Reaction 3a are equally vibrationally excited. The minimal-state correlation diagrams when all atoms lie on a plane (Cs symmetry), and when $O(^3P)$ approaches $O_3$ on the plane which bisects the $O_3$ bond angle, are shown in Fig. 4. In these cases, the correla-

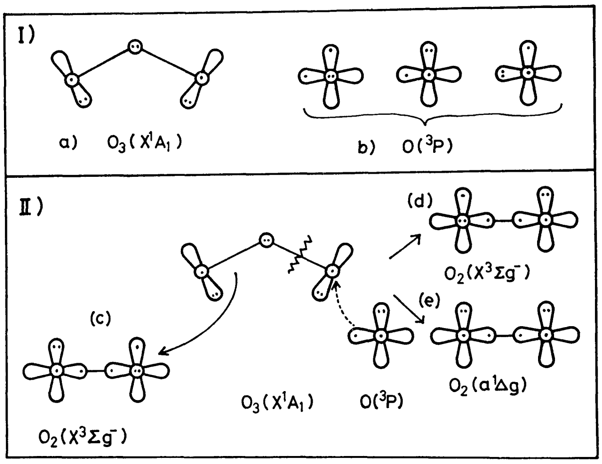

Fig. 5. GVB model representation in the $O+O_3$ reaction system.

tions with other upper states are abridged. As is shown in Fig. 4, the formation of the $a^1\Delta_g$-state molecular oxygen is possible in both the coplanar and bisecting plane models.

According to the valence-bond model which was explained by Goddard,[15] ground-state ozone and atomic oxygen are represented by (a) and (b) respectively in Fig. 5 (I). Figure 5 (II) shows the case in which an $O(^3P)$ approaches the side oxygen atom of ozone perpendicular to the ozone plane and in which each p-orbital having one electron makes a $\sigma$-bond. According to Goddard, this mechanism probably occurs in the lowest energy. In this case, $O_4$ in the transition state has no symmetry ($C_1$). When this $O_4$ complex is cleaved into two oxygen molecules, the electronic state of the $O_2$ on the left-hand side is in the ground state ($^3\Sigma_g^-$), while the $O_2$ in the right-hand side is the ground state (d) or the $a^1\Delta_g$ state (e). However, the O–O bond distance is expected to be shorter for the states with three oxygen $\pi$ electrons than for those with four $\pi$ electrons. This means that the energy of $O_4$ of the state of three $\pi$ electrons is lower than that of four electrons. Therefore, (d) in Case (II), the formation of the ground-state $O_2$, should give the lowest energy to the $O_4$ complex. It can be considered that the energy of the transition-state complex of $O_4$ is lowest in the case of the formation of two ground-state molecular oxygens (probably vibrationally excited) after cleavage.

2) *$H+O_3$ Reaction.* This reaction is wellknown as the source of the vibrationally excited OH radicals. Recent work[16] has shown that the OH-product vibrational distribution peaks strongly in the highest accessible vibrational level, $v=9$, and that the mean fractions of the total energy entering the vibration and rotation in the OH are $\langle f'v\rangle \approx 0.90$ and $\langle f'r\rangle \approx 0.03$.

$$H(^2S) + O_3(X^1A_1) \rightarrow OH(^2\pi) + O_2(X^3\Sigma_g^-) \quad (4a)$$

$$\Delta H = -76.9 \text{ kcal/mol}$$

However, OH is distributed in the lower levels, although it has progressively lower populations. Therefore, it is possible that singlet oxygen can be formed due to the exothermicity:

$$H(^2S) + O_3(X^1A_1) \rightarrow OH(^2\pi) + O_2^*(a^1\Delta_g) \quad (4b)$$

$$\rightarrow OH(^2\pi) + O_2^*(b^1\Sigma_g^+). \quad (4c)$$

There have been no reports on the singlet oxygen produced in the reaction of $H+O_3$. Measurements of the signals at mass number 32 were attempted by the method described above. The mass spectra measured in the $H+O_3$ reaction system are shown in Fig. 6. As is shown in Fig. 6, the signals at mass 32 are not changed in the $H+O_3+O_2$ and $H+O_2$ systems ($O_3/O_2$ was passed through the heater). The signals at mass 32 measured under a variety of $O_3/O_2$ concentrations are shown in Fig. 7. As is shown in Fig. 7, the signals for mass 32 did not increase in the presence of ozone. In this case, 4.6% of an $O_3/O_2$ mixture (without He as a diluent) was added. The concentration of ozone in the $O_3/O_2$ mixture and the absolute concentration of

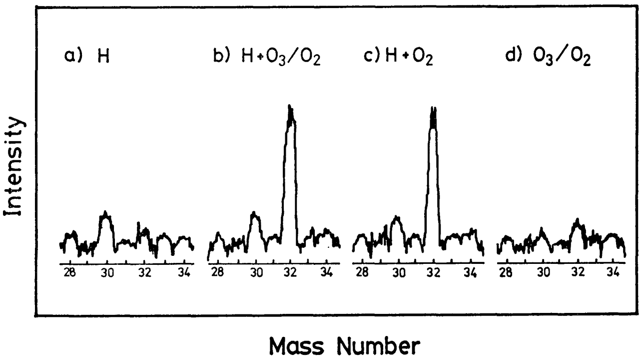

Fig. 6. Mass spectra in the $H+O_3$ reaction system.
a): Only $H_2$/He discharge. b): $O_3/O_2$ mixture was added to the $H_2$/He discharge. c): $O_3/O_2$ mixture was passed through the heated quartz tube. Ozone was converted to $O_2$. d): Discharge was turned off. Only $O_3/O_2$ mixture flowed. Conditions: total pressure=4.6 Torr, [H]=8.69 mTorr, $O_3+O_2=52$ mTorr, $O_3/O_2=7.5\%$, reaction time=6.1 ms.

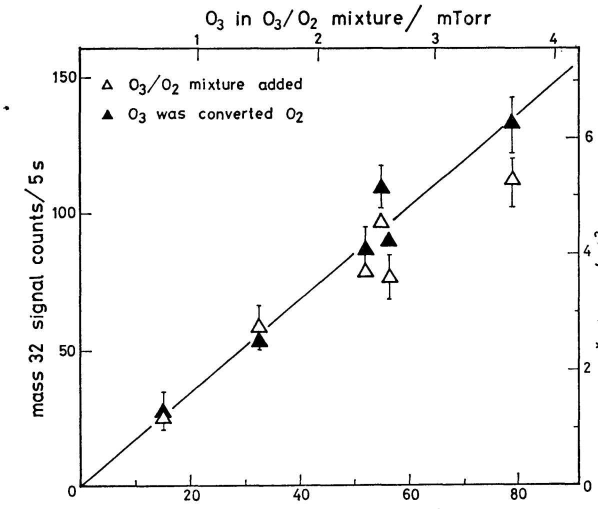

Fig. 7. Signals at $m/e=32$ *vs.* $O_3/O_2$ mixture added. △: Signals when $O_3/O_2$ mixture was added, ▲: signals when $O_3/O_2$ mixture was passed through the heated quartz tube. Conditions: total pressure=4.44 Torr, [H]=11.95 mTorr, reaction time=6.08 ms.

$O_2^*(a^1\Delta_g)$, as calculated from the sensitivity of NO, are shown in Fig. 7. When $O_3$ was converted to $O_2$ through the heater, the increase in the pressure of the $O_3/O_2$ mixture was about 2% ($O_3 \rightarrow 3/2O_2$). This is negligibly small compared with the counting error. The lack of increase in the signals for $O_2^*(a^1\Delta_g)$ in the presence of ozone showed that the $O_2^*(a^1\Delta_g)$ was formed only by Reactions 1 and 2. The absolute value for $O_2^*(a^1\Delta_g)$ agreed well with that of a previous work,[1)] in which the fraction of Reaction 2 was about 0.015 of the total reaction of $HO_2+H$.

The deactivation of $O_2^*(a^1\Delta_g)$ by $O_2$ and $O_3$ can be neglected during the contact time of this work, 6.08 ms. The deactivation rate constant of $O_2^*(a^1\Delta_g)$ by hydrogen atoms has been reported to be $2.5\times10^{-14}$ cm$^3$ molecule$^{-1}$ s$^{-1}$ [17)]. This rate was also slow enough to neglect under those conditions, [H]=11.95 mTorr. The deactivation rate of $O_2^*(a^1\Delta_g)$ by OH is unknown. However, the nearly linear increase in the $O_2^*(a^1\Delta_g)$ signal in the presence of $O_3$ in Fig. 7 shows that the deactivation of $O_2^*(a^1\Delta_g)$ by OH does not affect the $O_2^*(a^1\Delta_g)$ signals.

The rate constant for Reaction 1 previously reported[18)] is $1.57\times10^{-32}$ cm$^6$ molecule$^{-2}$ s$^{-1}$ (M=He). This means that the second-order rate for Reaction 1 is $2.3\times10^{-15}$ cm$^3$ molecule$^{-1}$ s$^{-1}$ under 4.44 Torr of He. On the other hand, the rate for Reaction 4 is very rapid. The rate constant for Reaction 4 was reported most recently[19)] to be $2.8\times10^{-11}$ cm$^3$ molecule$^{-1}$ s$^{-1}$ at 300 K. Therefore, the ozone should be consumed completely in the reactor under these experimental conditions, and the concentration of hydrogen atoms to react with $O_2$ might decrease with the addition of $O_3$. This effect is evident in Fig. 7. As is shown in Fig. 7, since the increment in the $1\times10^{-3}$ mTorr of $O_2^*(a^1\Delta_g)$ should be detectable in both the presence and absence of $O_3$, it was concluded that the fraction of the formation of $O_2^*(a^1\Delta_g)$, Reaction 4b, in the total reaction of $H+O_3$ must be less than 0.001.

The reaction of OH with $O_3$ produces $HO_2$:

$$OH + O_3 \rightarrow HO_2 + O_2. \qquad (5)$$

The rate constant for Reaction 5 reported most recently[20)] is $8.2\times10^{-14}$ cm$^3$ molecule$^{-1}$ s$^{-1}$ at 298 K. Three possible reaction paths have been suggested[21)] for the reaction of vibrationally excited OH with $O_3$:

$$\begin{aligned} OH^{\ddagger} + O_3 &\rightarrow HO_2 + O_2 && (6a)\\ &\rightarrow H + 2O_2 && (6b)\\ &\rightarrow OH + O + O_2. && (6c)\end{aligned}$$

The reactions of $OH^{\ddagger}$ ($v$=2—9) with $O_3$ have been shown to proceed with rate constants of (2—11)$\times10^{-12}$ cm$^3$ molecule$^{-1}$ s$^{-1}$ [21)]. These rates for Reaction 5 and 6 are not fast enough to compete with Reaction 4 under these experimental conditions ($[H]\gg[O_3]$).

In the correlation in the reaction of $H(^2S)+O_3(X^1A_1)$, the ground states $OH(X^2\pi)+O_2(X^3\Sigma_g^-)$, can be correlated through the $^2A'$-state $HO_3$ complex (in both Cs planar and Cs bisecting complex) to the $H(^2S)+O_3(X^1A_1)$. However the $OH(X^2\pi)+O_2^*(a^1\Delta_g)$ or $O_2^*(b^1\Sigma_g^+)$ can not be correlated to it. This fact is consistent with the finding of this experiment in which the production of singlet oxygen can not be observed and is a result of the production of highly vibrationally excited OH radicals.[16)]

*3) $NO+O_3$ Reaction.* The reaction of $NO+O_3$ is well known to emit the so-called "air afterglow" by means of the $NO_2$ formed, and this chemiluminescent reaction has been used by the chemiluminescent $NO_x$ analyzer:

$$NO(X^2\pi) + O_3(X^1A_1) \rightarrow NO_2(X^2A_1) + O_2(X^3\Sigma_g^-) \qquad (7)$$
$$\Delta H = -47.74 \text{ kcal/mol.}$$

In this case, the reaction produces visible and infrared emissions from electronically ($^2B_2$, $^2A_2$) and vibrationally excited ground-state $NO_2$.[22)] Recent works using seeded beams[23,24)] suggest that the cross-section of this chemiluminescent reaction increases very rapidly with an increase in the collision energy and is influenced by the electronic fine-structure states of NO ($\pi_{1/2}$, $\pi_{3/2}$). The enhancement of the reaction rate and chemiluminescence in this reaction by selective vibrational excitation with IR lasers has also been investigated.[25)]

A puzzling feature of the reaction is the failure to observe excited $O_2^*(a^1\Delta_g)$ and $O_2^*(b^1\Sigma_g^+)$, energetically accessible and favored by the correlation diagram, since $O_2^*(a^1\Delta_g)$ lies lower than any other excited states of $NO_2$. The failure to observe $O_2^*(a^1\Delta_g)$ has also been reported by Gauthier and Snelling[26)] in the reaction of $O_3$ with NO, where no $a^1\Delta_g$ emission was detected, and places an upper limit of 0.003 on the fraction of reactive collisions. A re-examination to observe

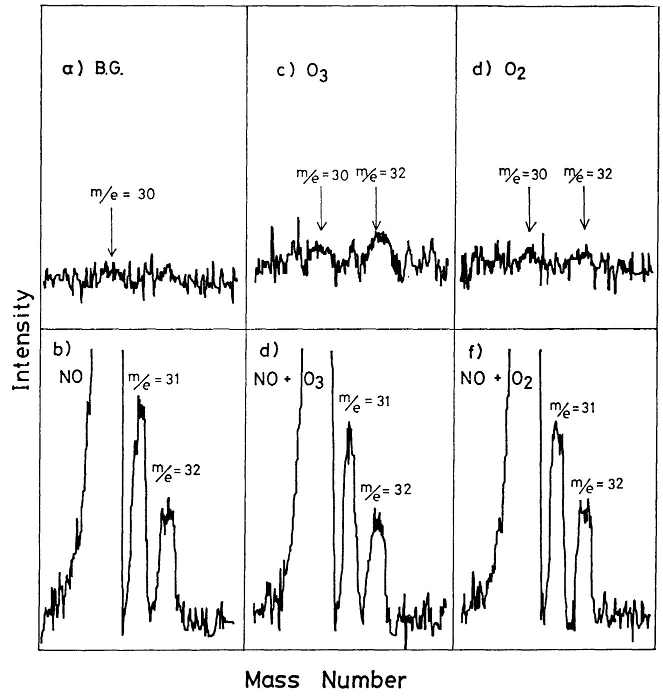

Fig. 8. Mass spectra in the $NO+O_3$ reaction system. a) Background. b) Only NO flowed. c) Only $O_3$–$O_2$–He mixture flowed. d) $NO+O_3$–$O_2$–He mixture. e) $O_3$–$O_2$–He mixture passed through the heated quartz tube. f) $NO+O_3$–$O_2$–He mixture passed through the heated quartz tube. Conditions: total pressure=3.8 Torr, $[O_3]$=18.2 mTorr, [NO]=2.3 mTorr, $[O_2]_i$=56.31 mTorr, reaction time=10.05 ms.

Table 2. Signals at $m/e=32$ in the $O_3+NO$ reaction system under these conditions total pressures$=3.782$ Torr, $[O_3]=18.23$ mTorr, $[NO]=2.30$ mTorr, $[O_2]_i=56.31$ mTorr, reaction time$=10.05$ ms

| Run | Condition | Mass 32 signal. counts/5 s averaged over 128 measurements | |
|---|---|---|---|
| A | Background | $28.9\pm 8.9$ | |
| B | Only $O_3$ | $31.7\pm 9.1$ | |
| C | Only $O_2$ (through heater) | $30.2\pm 9.8$ | |
| D | Only NO | $615.5\pm 27.8$ | |
| E | $O_3+NO$ | $561.2\pm 21.7$ | $E-B=529.5\pm 20.5$ |
| F | $O_2+NO$ (through heater) | $566.2\pm 25.7$ | $F-C=535.9\pm 24.3$ |

$O_2^*(a^1\Delta_g)$ was undertaken in the reaction of $O_3+NO$ by means of the photoionization mass spectrometer used in this study.

The mass spectra measured in the $NO+O_3$ reaction system are shown in Fig. 8. The signals at $m/e=32$ are overlapped by the isotope signals of NO. The signals accumulated at $m/e=32$ are shown in Table 2. The difference between the signals in the $O_3+NO$ (E—B) and $O_2+NO$ (F—C) reactions is $-6.44$ counts/5 s, which means that the increment in the signal at $m/e=32$ can not be observed in the $O_3+NO$ reaction. The rate constant for Reaction 7 reported most recently[27] is $1.80\times 10^{-14}$ cm$^3$ molecule$^{-1}$ s$^{-1}$ at 298 K. Therefore, the $O_2$ formed in Reaction 7 can be calculated to be $k_7[NO][O_3]t=0.250$ mTorr under the conditions listed in Table 2. On the other hand, 30 counts/5 s of the increment of the signal should be detectable under the conditions listed in Table 2 if $O_2^*(a^1\Delta_g)$ is produced. The 30 counts/5 s of the $O_2^*(a^1\Delta_g)$ signal can be calculated to be $4.8\times 10^{-4}$ mTorr because of the sensitivity of NO, $2.5\times 10^4$ counts/s for 1 mTorr. Therefore, the fraction for the formation of $O_2^*(a^1\Delta_g)$ in the total reaction of $O_3+NO$ should be less than 0.002.

The deactivation of $O_2^*(a^1\Delta_g)$ by NO and $NO_2$ have been reported[14] to be very slow, $4.5\times 10^{-17}$ and $5.0\times 10^{-18}$ cm$^3$ molecule$^{-1}$ s$^{-1}$ respectively. Therefore, the quenching of $O_2^*(a^1\Delta_g)$ by the reacting gases can be neglected. It has been suggested[2,28] that $O_2^*(a^1\Delta_g)$ can be formed in the energy-transfer reaction by electronically excited $NO_2$ with $O_2$.

$$NO_2^* + O_2 \rightarrow NO_2 + O_2^*(a^1\Delta_g). \qquad (8)$$

According to a report by Clough and Thrush,[22] the formation of electronically excited $NO_2$ emitting light shorter than 875 nm is 6.5% of the total reaction of $NO+O_3$ at 300 K. Jones and Bayes[2] have determined the efficiency for Reaction 8, which decreases from 3.5 to 0.5% as the $NO_2$ excitation wavelength increases from 420 to 620 nm. Therefore, if $NO_2^*$ is quenched completely only by $O_2$, the amount of $O_2^*(a^1\Delta_g)$ formed by Reaction 8 should be less than 0.002 of the total reaction of $NO+O_3$. Therefore, it is reasonable that the $O_2^*(a^1\Delta_g)$ produced in Reaction 8 could not be detected in this study. The above finding that less than 0.002 of the $NO+O_3$ reactive collisions result in the production of $O_2^*(a^1\Delta_g)$ is in good agreement with the result by Gauthier and Snelling.[26]

Redpath, Menzinger, and Carrington[23] preferred the bisecting-plane model in the $NO+O_3$ reaction, in which the NO approaches $O_3$ on the plane bisecting the $O_3$-bond angle (Cs symmetry); the formation of electronically excited $NO_2$ rather than the energetically preferred $O_2^*(a^1\Delta_g)$ can be explained by this model. However, the reaction on such a bisecting plane requires a very high energy, since ozone has the form of Ia) in Fig. 5.

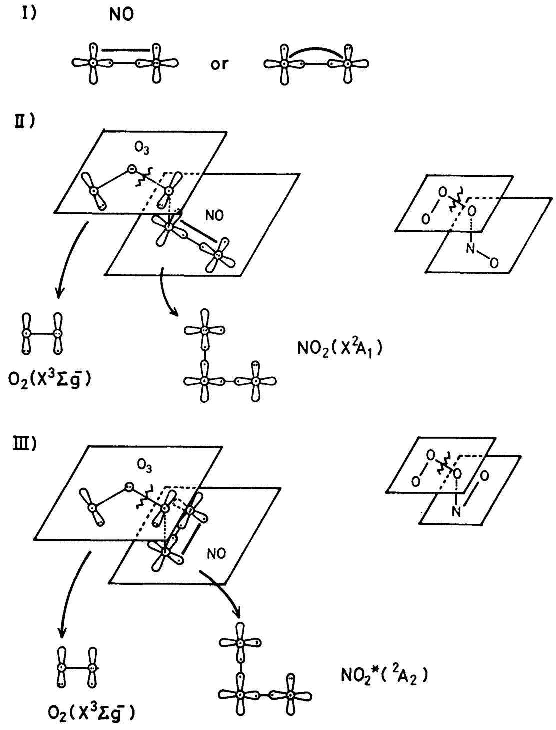

Fig. 9. GVB model representation in the $NO+O_3$ reaction system.

According to the GVB-model representation, the NO molecule is shown by I) in Fig. 9. The cases in which $O_3$ reacts with NO with the lowest energy are Cases (II) and (III) in Fig. 9. In these cases, NO approaches the side oxygen atom of $O_3$ parallel to the ozone plane and makes a N–O $\sigma$-bond perpendicular to the ozone plane. After this stage, the $NO_4$ complex cleavages to $O_2$ and $NO_2$. Two types of $NO_2$ are produced: $NO_2$ with $4\pi$ electrons, Case (II), corresponds to $NO_2(X^2A_1)$ and $NO_2^*(^2B_2)$, and that having $3\pi$ electrons, Case (III), corresponds to $NO_2^*(^2A_2)$ and $NO_2^*(^2B_1)$. Since it can be expected that molecules with a lower energy are predominantly produced, the

$NO_2$ formed in Case (II) should be in the ground state ($^2A_1$) while that in Case (III) should be in the $^2A_2$ state. On the other hand, the $O_2$ formed is in the ground state in both cases.

The formation of electronically excited $NO_2^*$ rather than the energetically preferred $O_2^*(a^1\Delta_g)$ can be explained by the GVB-model representation. However, the formation of the $^2B_1$ and the $^2B_2$ states of $NO_2$ can not be explained thus. It might be possible that the $^2B_1$ and the $^2B_2$ states of $NO_2$ are populated by vibronic interaction[29] with the $^2A_1$ and the $^2A_2$ states of the $NO_2$ produced initially after the $O_2$ has departed.

Further exact theoretical calculations are needed in order to clarify these reactions.

The authors wish to thank Professor Shigeru Nagase of Yokohama National University for his helpful discussions.

## References

1) N. Washida, H. Akimoto, and M. Okuda, *J. Phys. Chem.*, **82**, 18 (1978).

2) I. T. N. Jones and K. D. Bayes, *J. Chem. Phys.*, **59**, 3119 (1973).

3) J. R. Hislop and R. P. Wayne, *J. Chem. Soc., Fraday Trans. 2*, **73**, 506 (1977).

4) M. A. A. Clyne, "Physical Chemistry of Fast Reactions," ed by B.P. Levitt, Plenum Press (1973), Vol. 1, Chap. 4.

5) N. Washida, H. Akimoto, and M. Okuda, *J. Phys. Chem.*, **82**, 2293 (1978).

6) I. D. Clark and R. P. Wayne, *Mol. Phys.*, **18**, 523 (1970).

7) W. D. McGrath and R. G. W. Norrish, *Proc. R. Soc. London, Ser. A*, **242**, 265 (1957); W. D. McGrath and R. G. W. Norrish, *Nature*, **182**, 235 (1958); N. Basco and R. G. W. Norrish, *Can. J. Chem.*, **38**, 1769 (1960); W. M. Jones and N. Davidson, *J. Am. Chem. Soc.*, **84**, 2868 (1962); T. Carrington and D. Garoin, "Comprehensive Chemical Kinetics," ed by C. H. Barnford and C. F. H. Tipper, Elsevier Pub. (1969), Vol. 3, Chap. 4.

8) G. A. West, R. E. Weston, Jr., and G. W. Flynn, *Chem. Phys. Lett.*, **56**, 429 (1978).

9) D. D. Davis, W. Wong, and J. Lephardt, *Chem. Phys. Lett.*, **22**, 273 (1973).

10) J. L. McCrumb and F. Kaufman, *J. Chem. Phys.*, **57**, 1270 (1972).

11) I. D. Clark and R. P. Wayne, *Chem. Phys. Lett.*, **3**, 405 (1969).

12) I. D. Clark and R. P. Wayne, *Chem. Phys. Lett.*, **3**, 93 (1969); F. D. Findlay, C. J. Fortin, and D. R. Snelling, *Chem. Phys. Lett.*, **3**, 204 (1969); P. Borrell, P. M. Borrell, and M. D. Pedley, *Chem. Phys. Lett.*, **51**, 300 (1977); A. Leiss and U. Schurath, *J. Photochem.*, **8**, 211 (1978).

13) R. J. Collins, D. Husain, and R. J. Donovan, *J. Chem. Soc., Faraday Trans. 2*, **69**, 149 (1973).

14) K. H. Becker, W. Groth, and U. Schurath, *Chem. Phys. Lett.*, **8**, 259 (1971).

15) W. R. Wadt and W. A. Goddard, III, *J. Am. Chem Soc.*, **97**, 3004 (1975); P. J. Hay, T. J. Dunning, Jr., and W. A. Goddard III, *J. Chem. Phys.*, **62**, 3912 (1975); P. J. Hay and T. H. Dunning, Jr., *J. Chem. Phys.*, **67**, 2290 (1977); L. B. Harding and W. A. Goddard, III, *J. Am. Chem. Soc.*, **100**, 7180 (1978).

16) J. C. Polany and J. J. Sloan, *Int. J. Chem. Kinet. Symp.*, **1**, 51 (1975).

17) C. Schmidt and H. I. Schiff, *Chem. Phys. Lett.*, **23**, 339 (1973).

18) M. J. Kurylo, *J. Phys. Chem.*, **76**, 3518 (1972); W. Wong and D. D. Davis, *Int. J. Chem. Kinet.*, **6**, 401 (1974).

19) L. F. Phillips and H. E. Schiff *J. Chem. Phys.*, **37**, 1233 (1962); M. A. A. Clyne and P. B. Monkhouse, *J. Chem. Soc., Faraday Trans. 2*, **73**, 298 (1977); J. H. Lee, J. V. Michael, W. A. Payne, and L. J. Stief, *J. Chem. Phys.*, **69**, 350 (1978); L. F. Keyser, *J. Phys. Chem.*, **83**, 645 (1979).

20) A. R. Ravishankara, P. H. Wine, and A. O. Langford, *J. Chem. Phys.*, **70**, 984 (1979).

21) G. E. Streit and H. S. Johnston, *J. Chem. Phys.*, **64**, 95 (1976); R. N. Coltharp, S. D. Worley, and A. E. Potter, *Appl. Opt.*, **10**, 1786 (1971).

22) M. A. A. Clyne, B. A. Thrush, and R. P. Wayne, *Trans. Faraday Soc.*, **60**, 359 (1964); P. N. Clough and B.A. Thrush, *Trans. Faraday Soc.*, **63**, 915 (1967); P. N. Clough and B. A. Thrush, *Trans. Farday Soc.*, **65**, 23 (1969); M. F. Golde and F. Kaufman, *Chem. Phys. Lett.*, **29**, 480 (1974).

23) A. E. Redpath, M. Menzinger, and T. Carrington, *Chem. Phys.*, **27**, 409 (1978).

24) S. L. Anderson, J. Fite, O. V. Nguyen, and P. R. Brooks, "Molecular Beam Reaction of NO with $O_3$," Paper Presented at the ACS/CSJ Chemical Congress, Honolulu, Hawaii, April 1979; D. Van den Ende and S. Stolte, *Chem. Phys.*, **45**, 55 (1980).

25) M. J. Kurylo, W. Braun, A. Kaldor, S. M. Freund, and R. P. Wayne, *J. Photochem.*, **3**, 71 (1974); W. Braun, M. J. Kurylo, A. Kaldor, and R. P. Wayne, *J. Chem. Phys.*, **61**, 461 (1974); M. J. Kurylo, W. Braun, C. N. Xuan, and A. Kaldor, *ibid.*, **62**, 2065 (1975); **63**, 1042 (1975); R. J. Gordon and M. C. Lin, *ibid.*, **64**, 1058 (1976); J. Moy, E. Bar-Ziv, and R. J. Gordon, *ibid.*, **66**, 5439 (1977); *J.* C. Stephenson and S. M. Freund, *ibid.*, **65**, 4303 (1976); E. Bar-Ziv, J. Moy, and R. J. Gordon, *ibid.*, **68**, 1013 (1978); K. Hui and T. A. Cool, *ibid.*, **68**, 1022 (1978).

26) M. Gauthier and D. R. Snelling, *Chem. Phys. Lett.*, **20**, 178 (1973).

27) J. W. Birks, B. Schoemaker, T. J. Leck, and D. M. Hinton, *J. Chem. Phys.*, **65**, 5181 (1976).

28) T. C. Frankiewicz and R. S. Berry, *J. Chem. Phys.*, **58**, 1787 (1973).

29) J. C. D. Brand, W. J. Chan, and J. L. Hardwick, *J. Mol. Spectry.*, **56**, 309 (1975); C. G. Stevens and R. N. Zare, *ibid.*, **56**, 167 (1975); T. Tanaka, R. W. Field, and D. O. Harris, *ibid.*, **56**, 188 (1975).